JOURNAL OF ENZYME INHIBITION AND MEDICINAL CHEMISTRY
2022, VOL. 37, NO. 1, 1587–1599
https://doi.org/10.1080/14756366.2022.2081844

Taylor & Francis
Taylor & Francis Group

RESEARCH PAPER

Design, synthesis, molecular modeling and biological evaluation of novel Benzoxazole-Benzamide conjugates *via* a 2-Thioacetamido linker as potential anti-proliferative agents, VEGFR-2 inhibitors and apoptotic inducers

Ibrahim H. Eissa[a], Radwan El-Haggar[b,c], Mohammed A. Dahab[a], Marwa F. Ahmed[b,d], Hazem A. Mahdy[a], Reem I. Alsantali[d], Alaa Elwan[a], Nicolas Masurier[c] and Samar S. Fatahala[e]

[a]Pharmaceutical Medicinal Chemistry & Drug Design Department, Faculty of Pharmacy (Boys), Al-Azhar University, Cairo, Egypt; [b]Pharmaceutical Chemistry Department, Faculty of Pharmacy, Helwan University, Cairo, Egypt; [c]Institut des Biomolécules Max Mousseron (IBMM), UMR 5247, CNRS, Université de Montpellier, ENSCM, Montpellier, France; [d]Department of Pharmaceutical Chemistry, College of Pharmacy, Taif University, Taif, Saudi Arabia; [e]Pharmaceutical Organic Chemistry Department, Faculty of Pharmacy, Helwan University, Cairo, Egypt

ABSTRACT

A novel series of 2-thioacetamide linked benzoxazole-benzamide conjugates **1**–**15** was designed as potential inhibitors of the vascular endothelial growth factor receptor-2 (VEGFR-2). The prepared compounds were evaluated for their potential antitumor activity and their corresponding selective cytotoxicity was estimated using normal human fibroblast (WI-38) cells. Compounds **1**, **9**–**12** and **15** showed good selectivity and displayed excellent cytotoxic activity against both HCT-116 and MCF-7 cancer cell lines compared to sorafenib, used as a reference compound. Furthermore, compounds **1** and **11** showed potent VEGFR-2 inhibitory activity. The cell cycle progression assay showed that **1** and **11** induced cell cycle arrest at G2/M phase, with a concomitant increase in the pre-G1 cell population. Further pharmacological studies showed that **1** and **11** induced apoptosis and inhibited the expression of the anti-apoptotic Bcl-2 and Bcl-xL proteins in both cell lines. Therefore, compounds **1** and **11** might serve as promising candidates for future anticancer therapy development.

ARTICLE HISTORY
Received 25 February 2022
Revised 18 May 2022
Accepted 20 May 2022

KEYWORDS
Benzoxazole-benzamide; anti-cancer; apoptosis; VEGFR-2 inhibitors; Bcl-2

1. Introduction

Cancer is a lethal collection of diseases characterised by uncontrolled and overexcited cell differentiation and division mechanisms with the possibility to spread to or invade other parts of the body[1]. As a result, research work into anticancer medications that are highly effective and with minimal toxicity is still an important trend in anticancer drug research and development[2,3]. In this manner, many recent strategies targeting specific enzymes and/or biomarkers required for cancer cell proliferation and/or to control apoptosis such as mutated, deregulated, or overexpressed proteins[4] and thus, specifically affect cancer cells and/or their propping environment with the least effects on normal cells, attract major attention[5]. Among these targets are the vascular endothelial growth factor receptor-2 (VEGFR-2) which is one of the key intermediates in tumour angiogenesis[6], and the anti-apoptotic and pro-apoptotic proteins that regulate the cellular apoptosis[7–9].

Cancer cells need oxygen and nutrients to survive and proliferate; hence they must be near blood vessels to have accessibility to the blood circulation system[10]. Angiogenesis, the production of new blood capillaries from already existing vessels, is therefore an essential part in cancer growth and proliferation[11–13]. Accordingly, blocking angiogenesis through several methods including VEGFR-2 inhibition has proved significant effectiveness in cancer therapy[6]. Many studies have shown that inhibiting the VEGFR-2 or minimising its response is an efficient method in the assessment of new drugs for treatment of several cancer types[14–17].

Apoptosis, a mechanism of programmed cell death in multicellular organisms, is a chain of biochemical reactions that results in specific cell changes and cell death[18]. One of the main pathways of cell apoptosis induction is the mitochondria-dependent apoptotic pathway which is regulated by the B-cell lymphoma-2 (Bcl-2) protein family[19,20]. The Bcl-2 different family members could express opposite functions; some are pro-apoptotic proteins such as Bac and Bax, the two nuclear-encoded proteins that promote cell apoptosis, while others are anti-apoptotic proteins, such as Bcl-2 and Bcl-xL that inhibit cell apoptosis[9]. In this concern, it was reported that many cancer cells are characterised by the anti-apoptotic Bcl-2 protein overexpression that leads to apoptosis prevention as well as drug resistance[21,22]. Therefore, the production of Bcl-2 proteins inhibitors has become a significant target for introducing promising anti-cancer agents[23,24].

Recently, numerous small molecules bearing diversified heterocyclic scaffolds have been proved as potential anticancer agents *via* different mechanisms, including inhibition of angiogenesis

CONTACT Radwan El-Haggar radwan_elhaggar@pharm.helwan.edu.eg Department of Pharmaceutical Chemistry, Faculty of Pharmacy, Helwan University, Cairo 11795, Egypt; Alaa Elwan alaaelwan34@azhar.edu.eg Pharmaceutical Medicinal Chemistry & Drug Design Department, Faculty of Pharmacy (Boys), Al-Azhar University, Nasr, Cairo 11884, Egypt; Nicolas Masurier nicolas.masurier@umontpellier.fr Institut des Biomolécules Max Mousseron, Univ Montpellier, CNRS, ENSCM, 34293 MONTPELLIER cedex 5, France.

Supplemental data for this article is available online at https://doi.org/10.1080/14756366.2022.2081844.

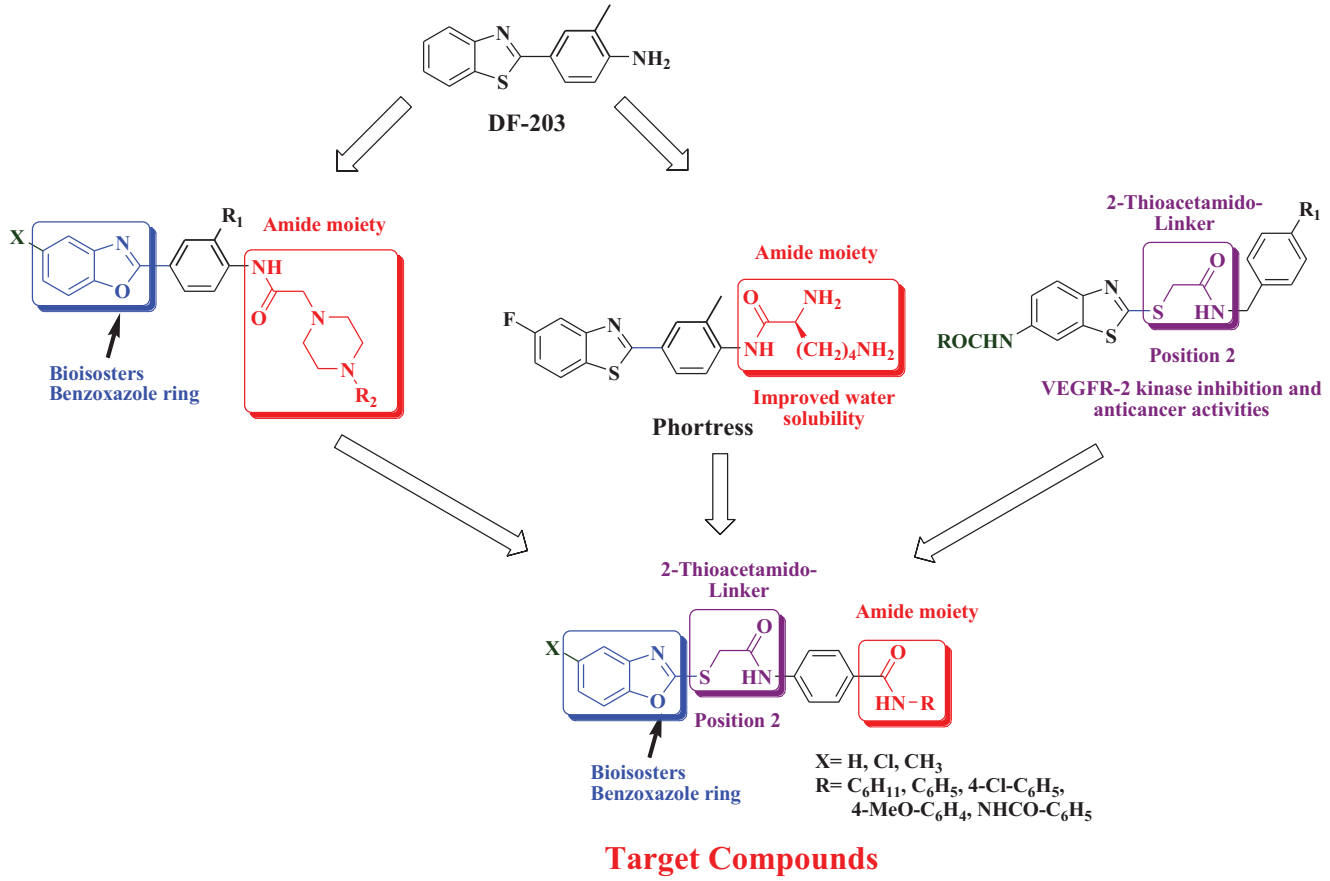

Figure 1. Design of the target benzoxazole-benzamide conjugates **1–15**.

and/or cell apoptosis induction[17]. For the meantime, the bicyclic isosteric scaffolds, namely; benzothiazole, benzoxazole and benzimidazole are considered as vital leads for many pharmacological activities including anti-inflammatory[25–29], antiviral[30–33], and mainly antitumor[34–45]. As a privileged scaffold, benzothiazole was the main nucleus for several compounds, such as compound **DF-203** (Figure 1) that showed significant *in-vitro* anticancer activities. However, its low solubility was the main issue for further *in-vivo* investigation[35]. **Phortress**, a water-soluble analog bearing an amino-acid moiety and displaying both strong and selective anticancer activity was developed to overcome these solubility difficulties[35] (Figure 1). An additional modification was conducted *via* replacing the benzothiazole ring with its benzoxazole bioisoster, which led to promising anticancer agents[43] (Figure 1). On the other hand, analogs with two aryl moieties separated with a 2-thioacetamido linker have been reported to have VEGFR-2 kinase inhibition, antitumor activity and improved aqueous solubility comparable to their lead compound[44].

Moreover, the novel benzoxazole series was designed to meet the four main pharmacophoric features reported for sorafenib and other VEGFR-2 inhibitors[46–48]. As illustrated in Figure 2 the proposed benzoxazole derivatives (**1–15**) exhibit pharmacophoric features similar to sorafenib, where the terminal benzoxazole ring could occupy the hinge region of the ATP binding site[47]. Also, the central aromatic benzene ring linked *via* a 2-thioacetamido group could occupy the area between the hinge region and the DFG domain of the activation loop[49]. In addition, the amide or diamide groups could act as H-bond donors and/or acceptors[50] and finally, the cyclohexyl or phenyl ring represents the terminal hydrophobic moiety that could occupy the allosteric hydrophobic pocket through several hydrophobic interactions[51] (Figure 2).

Considering the aforementioned findings, our group designed and synthesised a new series of benzoxazole-benzamide conjugates linked *via* a 2-thioacetamido moiety. All targeted compounds were evaluated *in-vitro* for their anticancer activity against both human breast (MCF-7) and colorectal (HCT-116) cancer cell lines and compared with their cytotoxicity in normal human fibroblasts (WI-38). For further investigation of the potential anticancer mechanism of the synthesised compounds, VEGFR enzymatic inhibition potential was determined, followed by DNA cell cycle analysis for the most active compounds. In addition, the ability of these conjugates to induce cell apoptosis was tested. The level of mitochondrial anti-apoptotic protein Bcl-2 and Bcl-xL in both HCT-116 and MCF-7 cancer cell lines was determined. Finally, molecular docking studies were performed for the synthesised compounds against VEGFR (PDB ID: 4ASD) with sorafenib as a reference ligand.

2. Results and discussion

2.1. Chemistry

Benzoxazole derivatives **1–15** were synthesised following the general methodologies outlined in Schemes 1 and 2. The key starting materials, 2-mercaptobenzoxazoles **IIa-c** were synthesised by refluxing the corresponding 2-aminophenol derivatives **Ia-c**, carbon disulphide, and potassium hydroxide in methanol, according to the reported procedure[52]. Then, compounds **IIa-c** were treated with alcoholic KOH to give the corresponding potassium salts, **IIIa-c** (Scheme 1). On the other hand, 4-aminobenzoic acid **IV** was reacted with chloroacetyl chloride in DMF to afford the chloroacetamide intermediate **V**. Then, treatment of compound **V** by

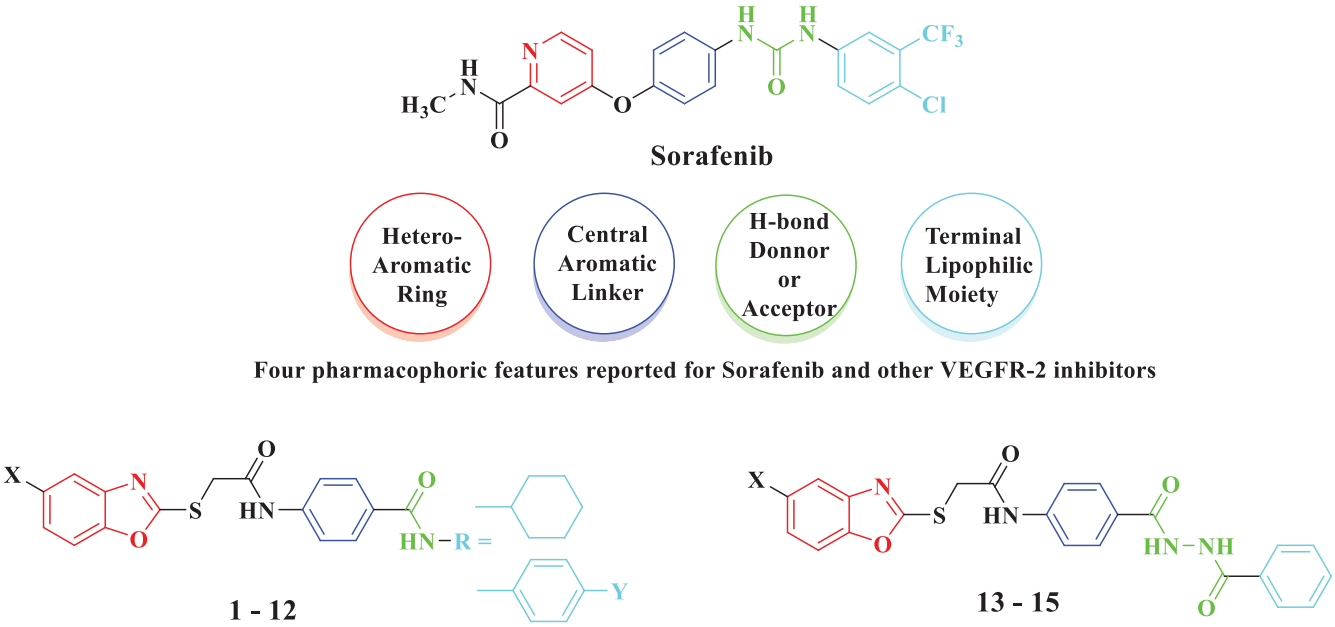

Figure 2. Target benzoxazoles fulfilled the pharmacophoric structural features of VEGFR-2 inhibitors.

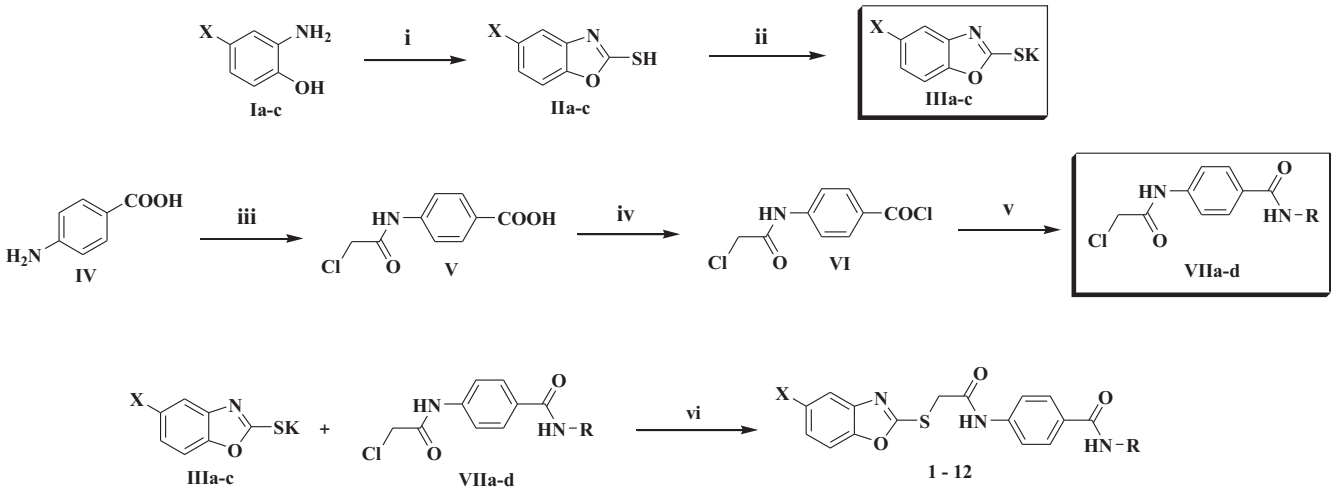

#	X	R	#	X	R	#	X	R
1	H	$-C_6H_{11}$	5	CH_3	$-C_6H_{11}$	9	Cl	$-C_6H_{11}$
2	H	$-C_6H_5$	6	CH_3	$-C_6H_5$	10	Cl	$-C_6H_5$
3	H	$-4\text{-}Cl\text{-}C_6H_4$	7	CH_3	$-4\text{-}Cl\text{-}C_6H_4$	11	Cl	$-4\text{-}Cl\text{-}C_6H_4$
4	H	$-4\text{-}OCH_3\text{-}C_6H_4$	8	CH_3	$-4\text{-}OCH_3\text{-}C_6H_4$	12	Cl	$-4\text{-}OCH_3\text{-}C_6H_4$

Scheme 1 Synthesis of the compounds **1–12**; Reagents/conditions: (i) CS_2/KOH/CH_3OH/reflux 6 h, (ii) KOH/C_2H_5OH/reflux 4 h, (iii) $ClCH_2COCl$, $NaHCO_3$/DMF/r.t./1h, (iv) $SOCl_2$/1,2-dichloroethane/reflux 4 h, (v) R-NH_2/acetonitrile/TEA/r.t. 8 h, (vi) DMF/KI/60 °C/6h.

thionyl chloride afforded 4-(2-chloroacetamido)benzoyl chloride **VI**[53,54], which was then successively reacted with a set of commercially available amines namely, cyclohexylamine, aniline, 4-chloroaniline, 4-methoxyaniline in acetonitrile and triethylamine (TEA), to get the key intermediates **VIIa-d**. Finally, compounds **VIIa-d** were heated with the formerly prepared potassium salts **IIIa-c** in dry DMF to afford the final target compounds **1–12** (Scheme 1).

On the other hand, methylbenzoate **IX** was prepared as reported, by refluxing benzoic acid **VIII** in methanol in presence of sulphuric acid[55,56]. Then, refluxing of **IX** with hydrazine hydrate afforded the corresponding acid hydrazide **X**[57], which was further acylated by **VI** in acetonitrile and TEA to afford the corresponding derivative **XI**. As previously, compound **IX** was finally heated with the formerly prepared potassium salts **IIIa-c** in dry DMF to afford the final target compounds **13–15** (Scheme 2).

The proposed structures of the final conjugates reported here were in full agreement with their elemental and spectral analysis data. IR spectra of all compounds displayed the absorption bands for the (NH) and (C=O) groups in the 3356–3273 and 1673–1598 cm^{-1} regions, respectively. Also, compounds **1**, **5** and **9** showed additional C-H stretching bands at 2933–2927 cm^{-1}, due to the presence of the aliphatic cyclohexyl group. In addition,

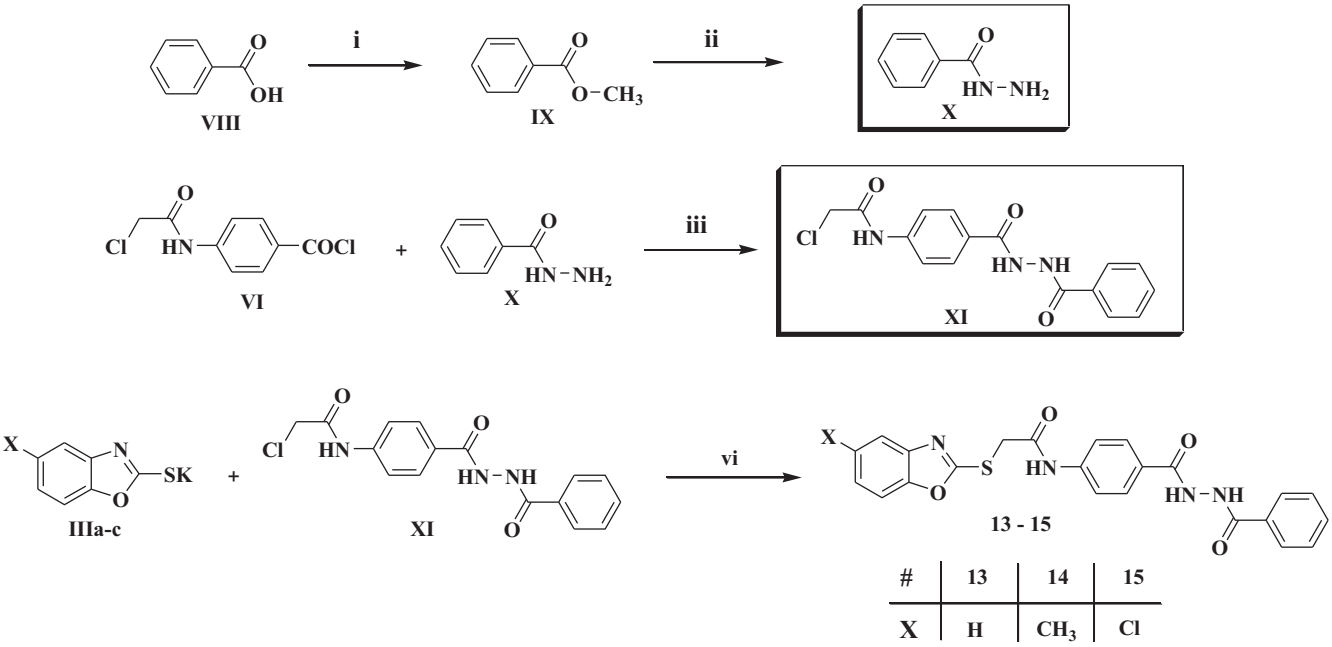

Scheme 2. Synthesis of the compounds **13–15**; Reagents/conditions: (i) CH_3OH/conc. H_2SO_4/reflux 2 h, (ii) NH_2-NH_2/C_2H_5OH/reflux 4 h, (iii) acetonitrile/TEA/r.t. 8 h, (vi) DMF/KI/60 °C/6h.

^{1}HNMR spectra for compounds **1**, **5** and **9** displayed two signals exchangeable with D_2O, referable to the two amidic NH groups at chemical shifts of δ 10.61–10.63 *ppm* and at δ 8.08 *ppm* for the acetamido group and benzamido group, respectively. For the remaining compounds, the signals of the two amidic NH groups were in the range of δ 10.68–10.73 *ppm* and at δ 10.00–10.24 *ppm* for the acetamido group and benzamido group, respectively. On the other hand, ^{1}HNMR spectra displayed the presence of a singlet peak for the methylene protons of the 2-thioacetamido linker at δ 4.37–4.43 *ppm*, whereas compounds **5**–**8** revealed another singlet peak in the aliphatic region referable to the methyl group at δ 2.37–2.28 *ppm*. Moreover, compounds **4**, **8** and **12** displayed an extra singlet signal for the methoxy group at δ 3.72 *ppm*.

Also, the structures of compounds **13**–**15** were confirmed by their spectral and elemental analyses. The ^{1}HNMR spectra for compounds **13**–**15** displayed three singlet signals exchangeable with D_2O, one for the acetamido group in the range of δ10.70–10.72 *ppm*, and two for the acyl hydrazide group at δ10.44 *ppm* and δ10.39 *ppm*. Additionally, the spectra showed a singlet signal for the methylene protons of the 2-thioacetamido linker in the range of δ 4.40–4.42 *ppm* for compounds **13**–**15** and a singlet signal attributed to the methyl group at δ 2.39 *ppm* for compound **14**.

2.2. Biological evaluation

2.2.1. Anti-proliferative activity against HCT-116 and MCF-7 human cancer cells lines

Recently, benzoxazole derivatives have attracted more attention in drug design, and notably to access compounds with anticancer activity. Several of these derivatives were reported as acting as competitive inhibitors of different tyrosine kinases, with potent cytotoxic activity against various cell lines[58,59]. Other series of benzoxazole derivatives showed significant potency against colon and breast cancer cell lines and their activity was explained by the potent inhibition of VEGFR enzymes[60–62]. Thus, in this study a novel series of benzoxazole-benzamide conjugates was initially evaluated for their potential anti-cancer activity against colon cancer cell line (HCT-116), breast cancer cell line (MCF-7) and normal human fibroblasts (WI-38), using the Sulforhodamine B colorimetric (SRB) assay[63]. Sorafenib as an FDA approved VEGFR-2 inhibitor was utilised as a positive reference compound. The cytotoxic activities were displayed in Table 1 and Figure 3 and expressed as the median growth inhibitory concentration (IC_{50}).

Table 1. *In vitro* anti-proliferative activity of the compounds **1–15** against HCT-116, MCF-7 human cancer cell lines and W-180 normal cell line, and their corresponding selectivity indices.

	HCT-116		MCF-7		WI-38
Compounds	IC_{50} (μM)[a]	SI[b]	IC_{50} (μM)[a]	SI[b]	IC_{50} (μM)[a]
1	7.8 ± 0.015	5.3	7.2 ± 0.010	5.8	41.9 ± 0.27
2	18.5 ± 0.014	3.0	11.7 ± 0.014	4.8	56.7 ± 0.36
3	24.2 ± 0.019	2.4	22.7 ± 0.008	2.6	59.3 ± 0.45
4	23.2 ± 0.012	2.2	23.6 ± 0.015	2.2	51.5 ± 0.40
5	20.9 ± 0.025	4.0	12.4 ± 0.007	6.9	85.4 ± 0.55
6	30.7 ± 0.011	4.0	19.1 ± 0.006	6.5	124.6 ± 0.70
7	32 ± 0.002	4.0	24 ± 0.011	5.3	128.2 ± 0.75
8	28.8 ± 0.010	4.7	22.3 ± 0.004	6.0	135.4 ± 0.85
9	17.1 ± 0.008	4.4	12.3 ± 0.008	6.0	74.6 ± 0.53
10	16.7 ± 0.012	7.5	16.1 ± 0.011	7.8	125.5 ± 0.72
11	12.2 ± 0.007	8.5	16.6 ± 0.013	6.2	103.5 ± 0.70
12	10.4 ± 0.010	12.1	9.4 ± 0.016	13.4	126.2 ± 0.75
13	9.1 ± 0.005	10.0	9.0 ± 0.005	10.1	91.3 ± 0.60
14	9.7 ± 0.013	9.9	9.5 ± 0.009	10.1	96.5 ± 0.65
15	12.9 ± 0.014	10.2	15.3 ± 0.01	8.6	131.5 ± 0.80
Sorafenib	11.6 ± 0.012	–	10.5 ± 0.014	–	–

[a]IC_{50} values are the mean ± SD of three separate experiments.
[b]Selectivity index (SI) is the ratio of the IC_{50} value for normal cells (WI-38) to the IC_{50} values for HCT-116 and MCF-7 cells.

Analysing results towards both HCT-116 and MCF-7 cell lines revealed that generally compounds bearing a 5-chlorobenzoxazole moiety (**9–12** and **15**) showed better cytotoxic activity than their 5-methyl (compounds **5–8** and **14**) or their unsubstituted benzoxazole analogs (compounds **2–4** and **13**), with the exception of compound **1**, bearing an unsubstituted benzoxazole moiety and a cyclohexyl group in its amidic side, and which displayed the best inhibitory activity of these two series, with IC_{50} values of

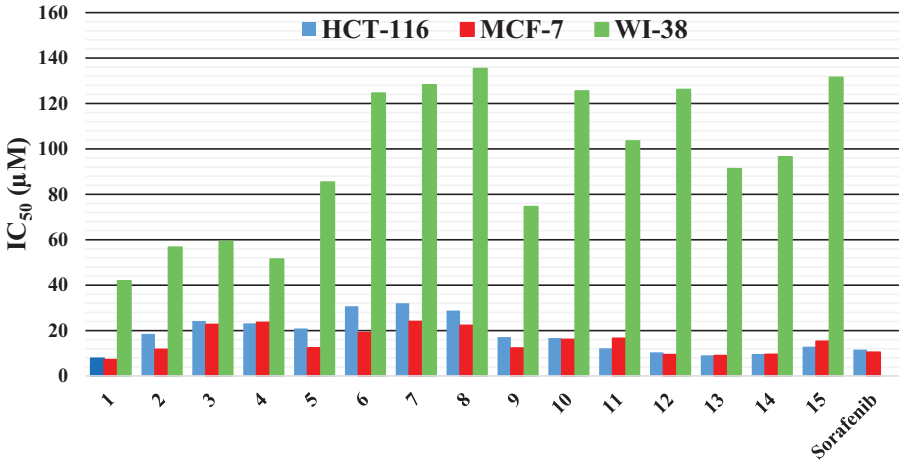

Figure 3. *In vitro* anti-proliferative activity of the target compounds **1–15**.

Table 2. Inhibitory activity of **1**, **9**, **10**, **11**, **12** and **15** against VEGR-2 Protein Kinase.

No.	VEGFR-2 Protein Kinase IC_{50} (µM)
1	0.268 ± 0.005
9	0.649 ± 0.008
10	0.704 ± 0.009
11	0.361 ± 0.004
12	0.385 ± 0.005
15	0.597 ± 0.007
Sorafenib	0.352 ± 0.005

IC_{50} values are the mean of three individual experiments.

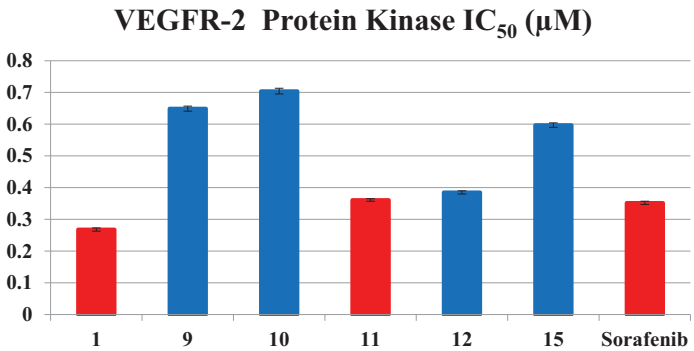

Figure 4. Inhibitory activity of **1**, **9**, **10**, **11**, **12** and **15** against VEGR-2 Protein Kinase.

7.2 ± 0.01 µM and 7.8 ± 0.015 µM against HCT-116 and MCF7 cell lines, respectively. Concerning the influence of the amide group, a cyclohexyl substituent led globally to more active compounds than a phenyl or a substituted phenyl group (compared compounds **1** to **2**–**4** or **5** to **6**–**8** or **9** to **10**), except for compound **12** bearing a 4-methoxybenzamide group, which was more active than its cyclohexyl analog **9**. Moreover, it is worthy to mention that generally the acyl hydrazide derivatives **13–15** showed higher inhibitory activity than their benzamide analogs towards both cancer cell lines. Thus, as an example, compound **13** showed an IC_{50} of 9.1 ± 0.005 µM against HCT-116 cells, compared to an IC_{50} of 18.5 ± 0.005 µM for compound **2**.

In addition, results against the MCF-7 cell line showed that compounds **1** and **12**–**14** exhibited excellent activity with single-digit micromolar IC_{50} values ranged between 7.2 ± 0.01 and 9.5 ± 0.009 µM, more potent than the reference drug, sorafenib. While compounds **2**, **5** and **9** showed good potency with IC_{50} of 11.7 ± 0.014−12.4 ± 0.007 µM, the remaining compounds had moderate to weak cytotoxic activity with IC_{50} of 15.3 ± 0.01−24.0 ± 0.011 µM. In a similar way, compounds **1**, **12–14** showed a single digit micromolar IC_{50} values against HCT-116 cells (IC_{50} range: 7.8 ± 0.015−10.4 ± 0.01 µM), higher than sorafenib that possessed IC_{50} value of 11.6 ± 1.00 µM. On the other hand, while compounds **11** and **15** showed good potency with IC_{50} values of 12.2 ± 0.007−12.9 ± 0.014 µM, the remaining compounds had moderate to weak cytotoxic activity with IC_{50} range of 16.7 ± 0.012−32.0 ± 0.002 µM.

Finally, all tested compounds showed weak cytotoxicity against normal human fibroblasts (WI-38), with IC_{50} range of 42−135 µM, representing a selectivity index of 2.2 to 13.4, compared to IC_{50} values against both HCT-116 and MCF-7 cancer cell lines.

Table 3. Effect of compounds **1**, **11** and vehicle control on the cell cycle phases of HCT-116 and MCF-7 cells lines.

Compound / Cell line	%G0-G1	%S	%G2-M	%Pre-G1
1 / HCT116	42.34	33.25	24.41	15.36
11 / HCT116	45.37	26.19	28.44	17.41
Control / HCT116	49.51	31.56	18.93	4.52
1 / MCF7	40.66	29.72	29.62	19.78
11 / MCF7	43.84	30.92	25.24	16.93
Control / MCF7	55.14	28.33	16.53	3.41

These results revealed that some of the novel benzoxazole compounds are very promising candidates as relatively safe cytotoxic agents. Thus, the most active derivatives were submitted for further investigations regarding their potential anti-proliferative mode of action.

2.2.2. VEGFR-2 inhibitory activity

The excellent cytotoxic effects of several benzoxazole derivatives, in particular compound **1**, motivated a further exploration of their potential inhibitory activities against VEGFR-2 protein kinase. Representative compounds **1**, **9**–**12** and **15** were selected to determine their potential inhibitory activity. As presented in Table 2 and Figure 4, the results revealed that all examined compounds exhibited sub-micromolar IC_{50} values of VEGFR-2 inhibitory activity. Among all tested compounds, the unsubstituted benzoxazole compound **1**, bearing a cyclohexyl group in the amidic side, was the best inhibitor of VEGFR-2 activity with IC_{50} value of 0.268 µM, more potent than the clinically used kinase inhibitor, sorafenib, which exhibited IC_{50} value of 0.352 µM, followed by conjugates **11** and **12** with comparable IC_{50} values of 0.361 µM and 0.385 µM,

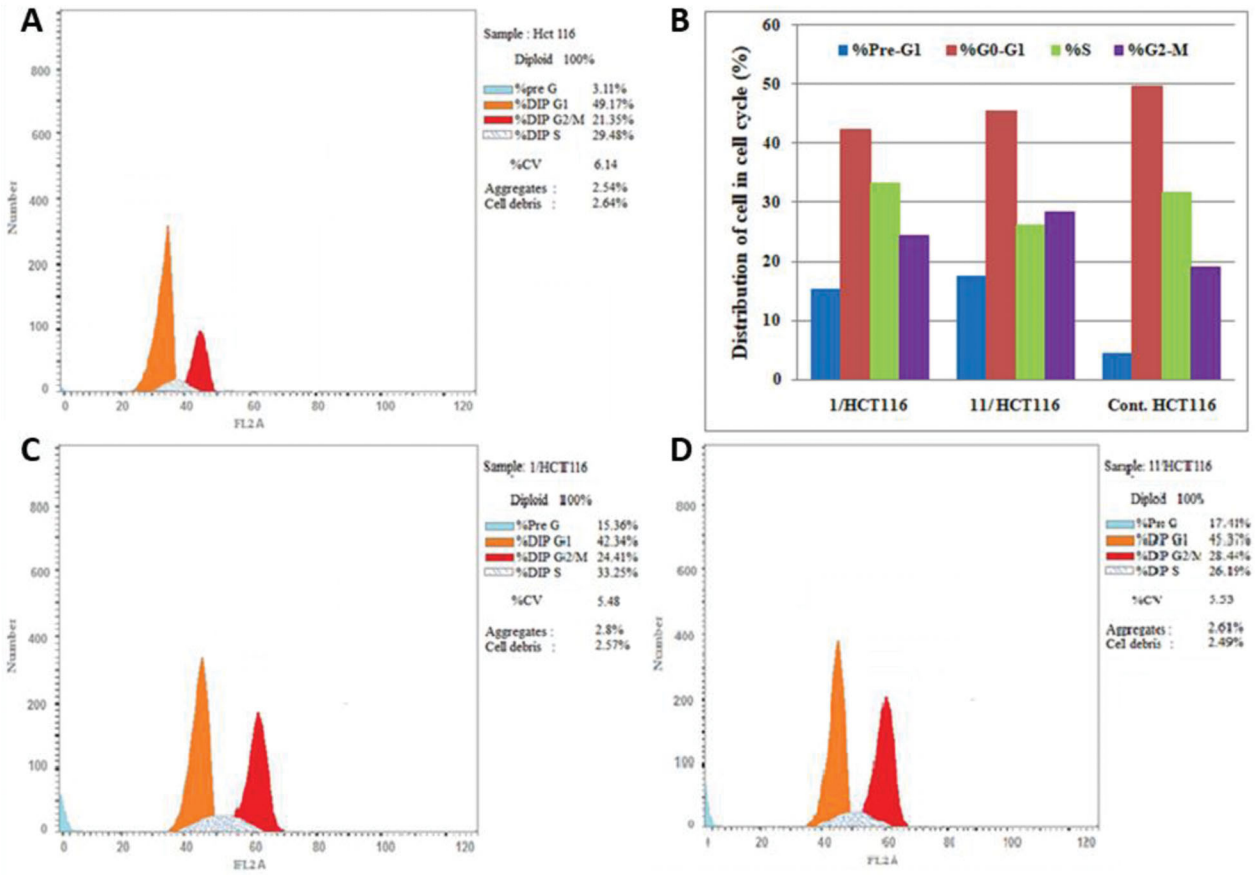

Figure 5. Cell distribution in the subG1, G0/G1, S and G2/M phases for HCT116 cells (**B**) treated with vehicle control (**A**), compounds **1** (**C**) and **11** (**D**).

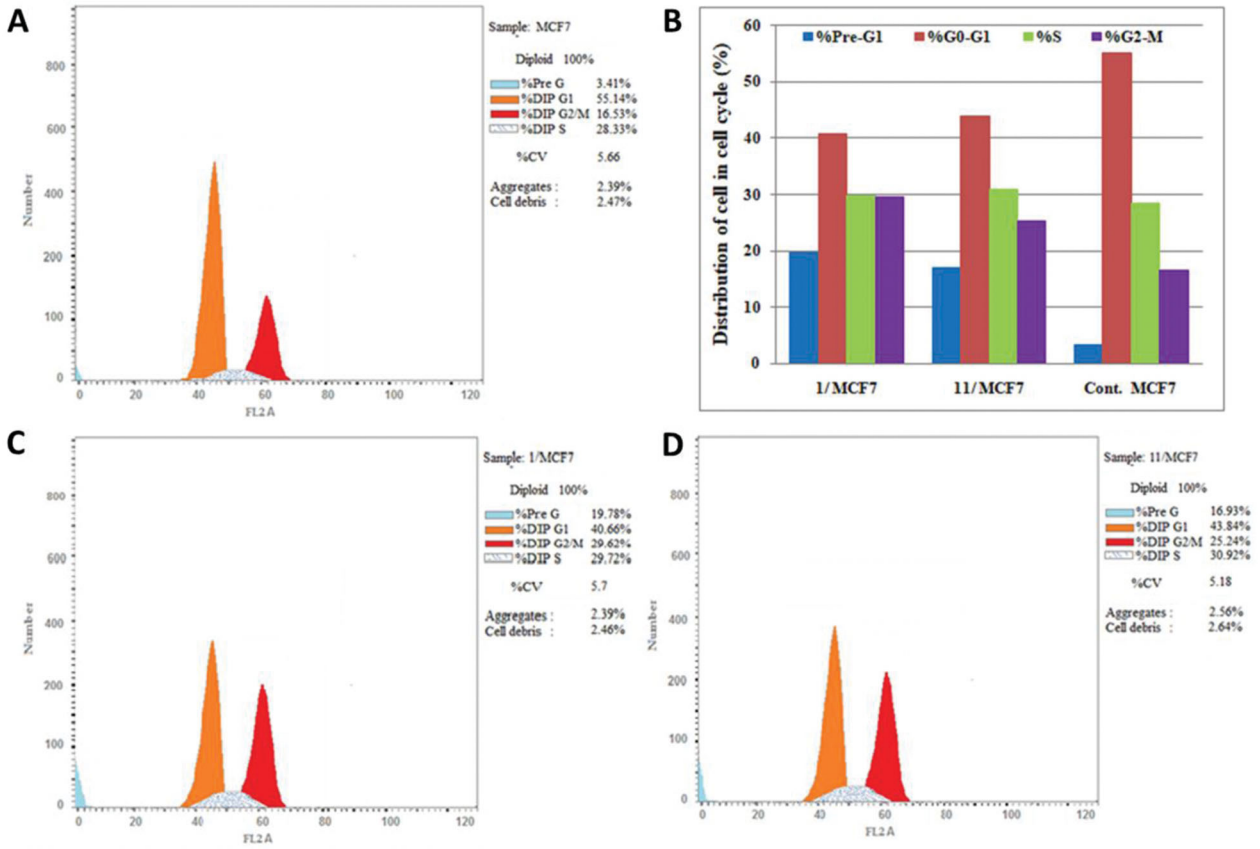

Figure 6. Cell distribution in the subG1, G0/G1, S and G2/M phases for MCF7 cells (**B**) treated with vehicle control (**A**), compounds **1** (**C**) and **11** (**D**).

respectively. On the other hand, compounds **9**, **10** and **15** exhibited the least inhibitory activity with IC_{50} value ranged from 0.597 to 0.704 µM. Finally, the presented results revealed that the VEGFR-2 inhibitory activities were in excellent match with the cytotoxic activities of compounds **1**, **11** and **12** suggesting that the anti-proliferative activity might be attributable to VEGFR-2 enzyme inhibition.

2.2.3. Cell cycle analysis

It is clearly known that generally the cytotoxic agents exert their anti-proliferative effect *via* cell cycle arrest at a specific phase. In the present study, due to the excellent *in-vitro* anti-proliferative activity of conjugates **1** and **11** against both HCT-116 and MCF-7 cancer cell lines as well as their excellent VEGFR-2 inhibitory activities, cell cycle analysis have been carried out for both compounds. The effect of compounds **1** and **11** on the cell cycle progression in order to determine the phase at which cell cycle arrest takes place in both cancer cell lines was evaluated by a DNA flow cytometry analysis, upon incubation of HCT-116 and MCF-7 cancer cell lines with compounds **1** and **11** at their IC_{50} concentrations for 24 h (Table 3 and Figures 5 and 6).

The results showed that, for HCT-116 cancer cells lines, the percentage of cells at G2/M phase relatively increased from 18.93% in control to 24.41% and 28.44% after incubation with compounds **1** and **11**, respectively. In addition, the percentage of HCT-116 cells in G1 phase was decreased from 49.51% to 42.34% for compound **1** and 45.37% for compound **11** (Figure 5).

Similarly, the results revealed that, for MCF-7 cancer cell line, the percentage of cells in the G2/M phase was significantly increased from 16.53% to 29.62% for compound **1** and 25.24% for compound **11**. In addition, the percentage of MCF-7 cells at G1 phase decreased from 55.14% in control to 40.66% and 43.84% after incubation with compounds **1** and **11**, respectively (Figure 6). These results indicated that compounds **1** and **11** induced cell cycle arrest at G2/M phase. Finally, the upsurge of cell populations in the pre-G1 phase along with the G2-M phase arrest were significant evidence that compounds **1** and **11** induced apoptosis in both HCT-116 and MCF-7 cancer cell lines.

Table 4. Percent of apoptosis and necrosis induced by compounds **1**, **11** and vehicle control in HCT-116 and MCF-7 cell lines.

	%Apoptosis			
Compound / Cell line	%Total	%Early	%Late	%Necrosis
1 / HCT-116	15.36	4.86	8.95	1.55
11 / HCT-116	17.41	6.01	9.62	1.78
Control / HCT-116	4.52	1.1	1.57	1.85
1 / MCF-7	19.78	6.02	12.17	1.59
11 / MCF-7	16.93	4.93	10.26	1.74
Control / MCF-7	3.41	0.47	1.34	1.6

2.2.4. Annexin V-FITC/PI apoptosis test

To determine whether the growth inhibitory action of compounds **1** and **11** is consistent with the induction of apoptosis suggested

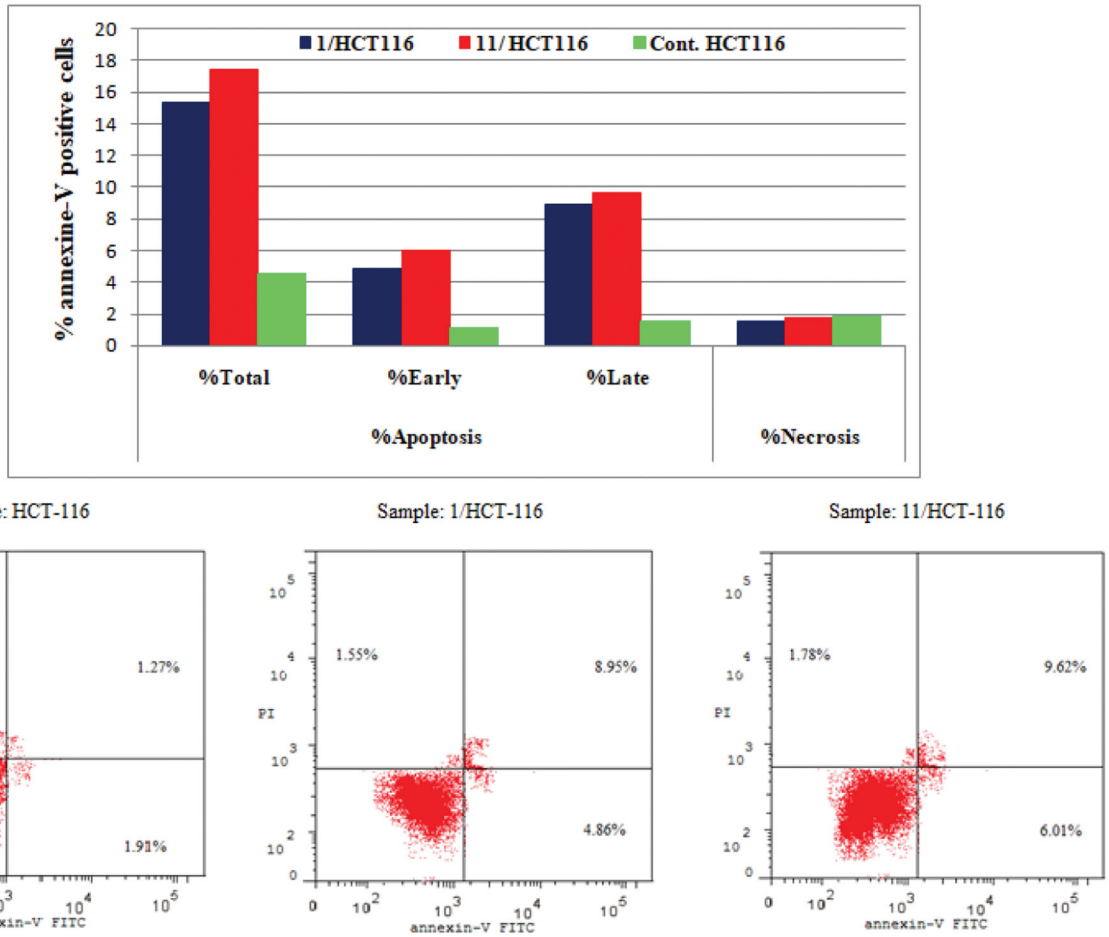

Figure 7. Effect of compounds **1**, **11** and vehicle control on the percentage of annexin V-FITC-positive staining in HCT-116 cell line. The experiments were done in triplicates. The four quadrants identified as: LL, viable; LR, early apoptotic; UR, late apoptotic; UL, necrotic.

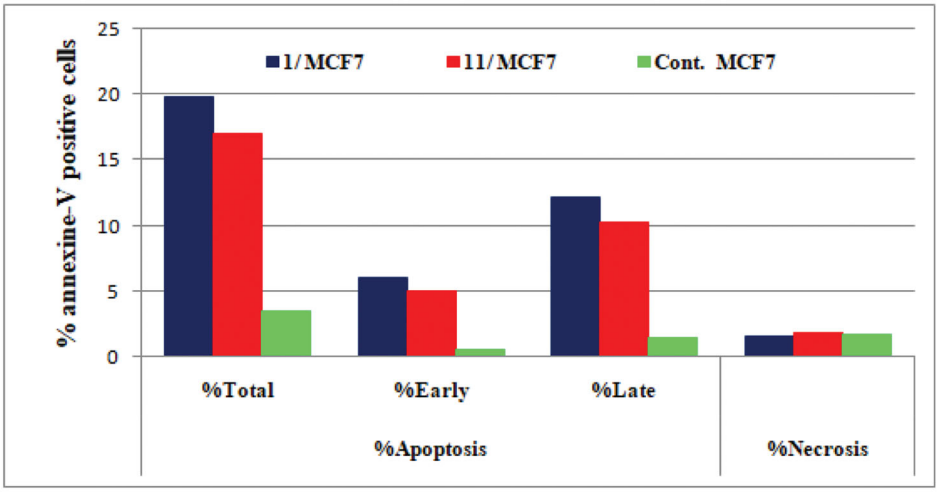

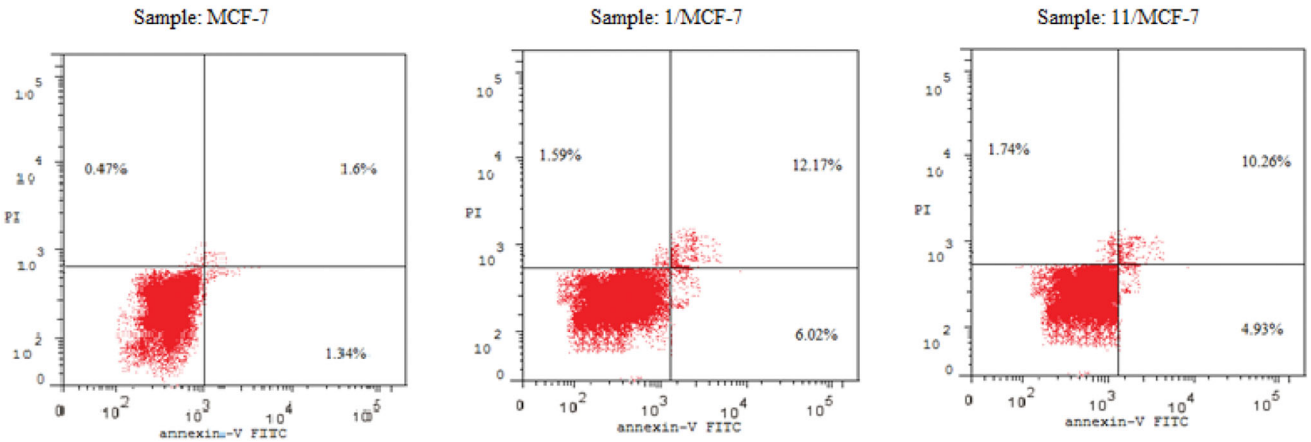

Figure 8. Effect of compounds **1**, **11** and vehicle control on the percentage of annexin V-FITC-positive staining in MCF-7 cell lines. The experiments were done in triplicates.

by the elevated population of pre-G1 in the treated HCT-116 and MCF-7 cells, Annexin V-FITC/PI double staining (AV/PI) apoptosis assay was carried out. The results of this assay revealed that compounds **1** and **11** induced both early and late apoptosis in both HCT-116 and MCF-7 cell lines and the results were outlined in Table 4 and Figures 7 and 8.

The results revealed that treatment of HCT-116 cells with compound **1** and **11** resulted in an increase in the apoptotic cells percentage for the early apoptosis, from 1.1% for control untreated cells to 4.89% and 6.01%, respectively. In addition, the percentage of apoptotic cells in the late stage was 8.95% to 9.62% compared to control (1.57%). These results revealed that compounds **1** and **11** were able to induce an approximately 3.4-folds and 3.9-folds, respectively, increase in total apoptosis compared to the control for HCT-116 cell line (Figure 7).

On the other hand, for MCF-7 cancer cell line, the results showed that conjugates **1** and **11** led to an increase in the apoptotic cells percentage for the early apoptosis, from 0.47% for control untreated cells to 6.02% and 4.93%, respectively. In addition, for the late stage, the percentage of apoptotic cells increased from 1.34% for control cells to 12.17% and 10.26%, for compounds **1** and **11,** respectively. These results showed that the tested compounds were able to induce an approximately 5.8-fold and 5.0-fold total increase in apoptosis compared to the control, for compounds **1** and **11** respectively (Figure 8). These results persuaded us to further investigate the effect of compound **1** and **11** on mitochondrial anti-apoptotic biomarkers Bcl-2 and Bcl-xL.

2.2.5. Impact of compounds 1 and 11 on the level of Bcl-2 and Bcl-xL

It is well known that the anti-apoptotic proteins Bcl-2 and Bcl-xL are mainly overexpressed in various types of cancer, causing survival of cancer cells and/or drug resistance[7–9]. Therefore, inhibition of these proteins expression leads to cancer cell death and has been used as a strategy for anticancer drug development[23]. In this study, the impact of compounds **1** and **11** on Bcl-2 and Bcl-xL expression in HCT-116 and MCF-7 cancer cell lines was examined using Western blot analysis and all the data were normalised to β-actin (Figure 9). The presented results revealed that benzoxazoles **1** and **11** inhibited Bcl-2 and Bcl-xL expression in both HCT-116 and MCF-7 cancer cell lines in a corresponding manner to their cytotoxic activity and their apoptosis induction ability.

2.2.6. Molecular docking

Molecular docking studies are considered as an influential method for interpretation of molecular interactions between the synthesised compounds and the main amino acid residues at the specific

Table 5. Docking energy scores (kcal/mol) obtained from the MOE software for compounds **1–15** and sorafenib.

Compound No.	Score	rmsd_refine	E_conf	E_place	E_score1	E_refine	E_score2
1	−8.45083	3.46348	7.13944	−61.18144	−10.73645	−15.61404	−8.450831
2	−8.07490	4.14820	24.33731	−65.02733	−11.56395	−16.29065	−8.074901
3	−7.18548	1.39598	29.55076	−82.09853	−11.23328	−8.114554	−7.185479
4	−8.41887	1.47159	27.91452	−89.37426	−11.65076	−19.99584	−8.418868
5	−7.63854	2.33253	2.78024	−88.87581	−12.35492	−4.167041	−7.638539
6	−7.88400	1.76917	20.26365	−77.02324	−11.26872	−15.04636	−7.884004
7	−9.36350	1.7113	17.05548	−84.28175	−11.35441	−22.20009	−9.363497
8	−9.38409	1.46039	21.96994	−79.49125	−12.83700	−22.23286	−9.384088
9	−7.93492	0.97358	−1.62790	−108.53313	−12.54650	−5.27634	−7.934922
10	−8.69645	2.34028	9.40272	−69.44931	−11.03539	−21.76292	−8.696453
11	−8.15044	3.47698	16.16184	−104.55356	−11.93168	−16.78374	−8.150444
12	−9.30653	2.37350	11.61155	−100.80922	−11.70867	−21.75587	−9.306530
13	−8.82812	1.14095	63.19030	−79.27531	−10.92340	−23.19646	−8.828117
14	−8.71854	2.22981	70.10210	−86.90809	−10.84697	−21.77860	−8.718533
15	−9.27842	1.94674	53.63672	−69.43458	−10.36066	−21.94845	−9.278418
Sorafenib	−6.98449	1.78143	−3.12607	−79.69516	−10.28793	−7.641235	−6.984490

Score: lower scores are more favourable; **rmsd_refine**: the root mean square deviation of the pose; **E_conf**: free binding energy (**FBE**) of the conformer; **E_place**: **FBE** from the placement stage; **E_score 1**: **FBE** from the first rescoring stage; **E_refine**: **FBE** from the refinement stage; **E_score 2**: **FBE** from the second rescoring stage.

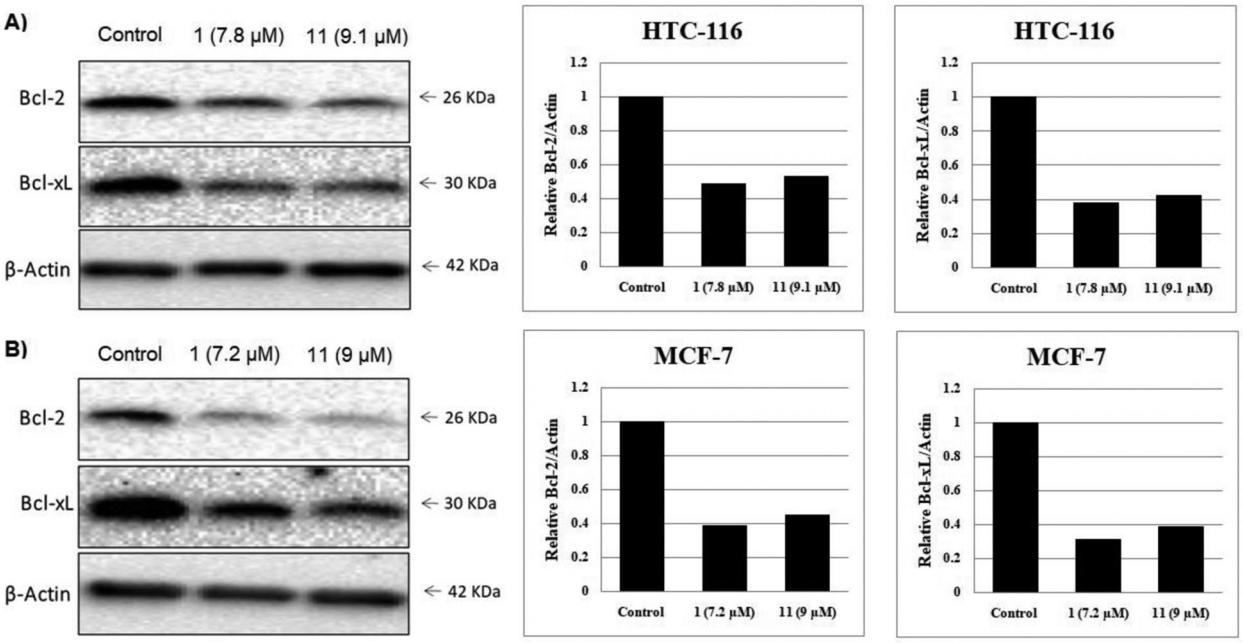

Figure 9. Effect of compounds **1**, **11** and vehicle control on anti-apoptotic proteins (Bcl-2 and Bcl-xL) in (**A**) HCT-116 cancer cells and (**B**) MCF-7 cancer cells.

binding site of the target receptor[64]. The activity of the newly synthesised ligands and VEGFR protein interactions at the active binding site was compared according to the docking score values calculated using MOE 2015.10. In the current work, all the synthesised benzoxazole compounds were put through molecular docking studies using MOE software on the VEGFR 3D-structure and using sorafenib as a reference ligand.

The results revealed that, the most biologically active compounds **1** and **11** displayed an excellent docking score (−8.45083 kcal/mol and −8.15044 kcal/mol, respectively) compared to sorafenib docking score (−6.98449 kcal/mol), and both compounds formed direct interactions with many of the amino-acids that sorafenib interacted with (Table 5). As shown in Figure 10, sorafenib had direct interactions with amino-acids Leu840, Glu885, Lys920 and Asp1046 in the active site (Figure 10(A)). Compound **1** shared sorafenib interactions with amino-acids Leu840 and Asp1046, and additionally exhibited other interactions with amino-acids Lys868, Cys919 and Phe1047 (Figure 10(B)). On the other hand, compound **11** shared the interaction with only Asp1046 and showed another interaction with amino-acid Lys868 (Figure 10(C)). Also, compounds **1** and **11** displayed high degrees of superimposition with sorafenib into the VEGFR active site (Figure 10(B,C)). Finally, the more interaction formed with amino-acids at the active site by compound **1** than compound **11** strongly support the results of VEGFR enzyme inhibition assay where compound **1** was the most active with IC_{50} of 0.268 μM compared to that of compound **11** and sorafenib that had IC_{50s} of 0.361 μM and 0.352 μM, respectively (Table 2).

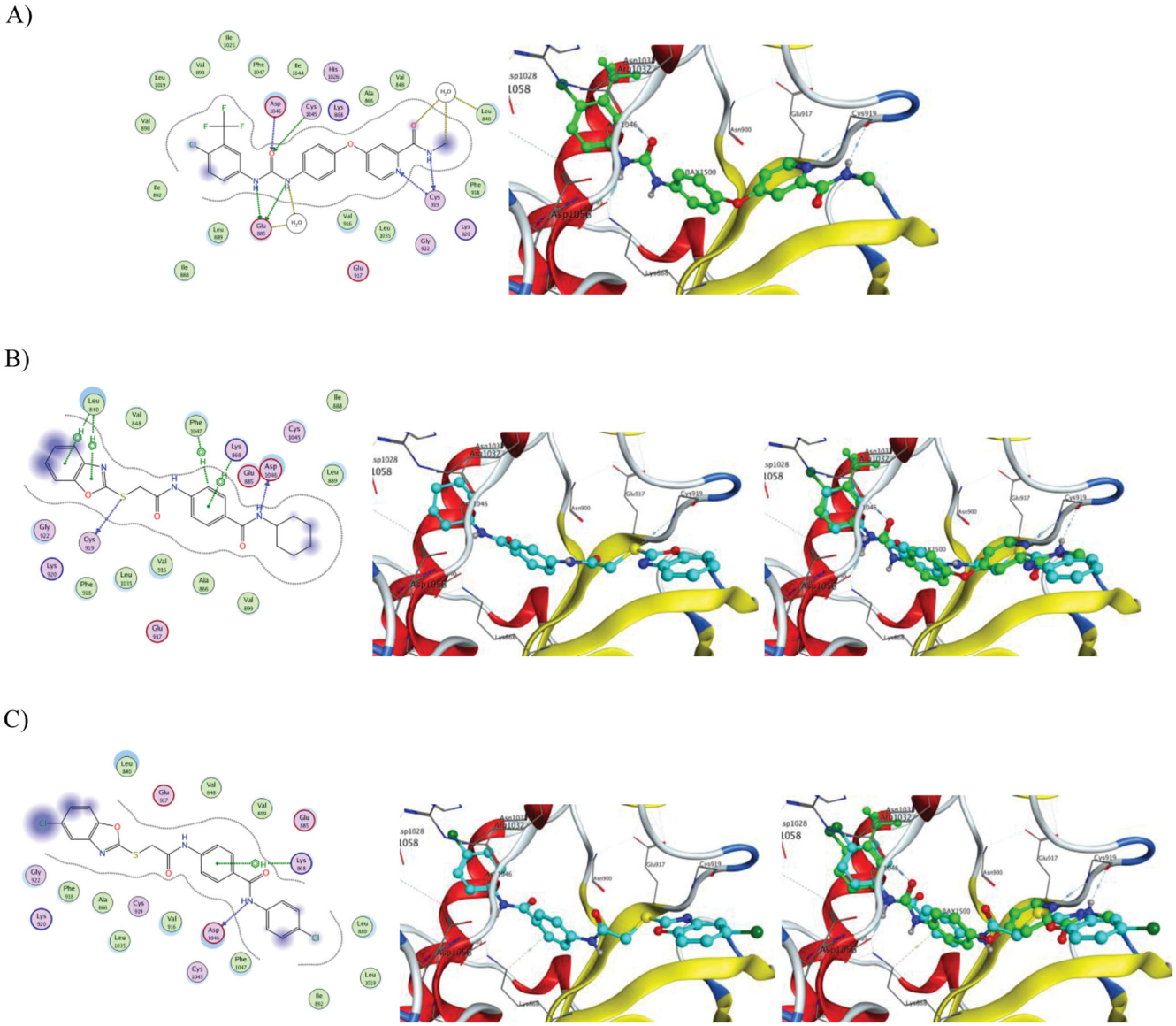

Figure 10. Docking of compounds **1**, **11** and sorafenib into the VEGFR active site. (A) Interaction of Sorafenib with amino-acids Leu840, Glu885, Lys920 and Asp1046. (B) Interaction of **1** with amino-acids Leu840, Lys868, Cys919, Asp1046 and Phe1047 and superimposition of **1** (shown as cyan sticks) with sorafenib (shown as green sticks). (C) Interaction of **11** with amino-acids Lys868 and Asp1046 and superimposition of **11** (shown as cyan sticks) with sorafenib (shown as green sticks).

3. Conclusions

In the current study, a novel series of novel benzoxazole-benzamide conjugates linked *via* a 2-thioacetamido group (**1**−**15**) was designed and synthesised as potential anti-cancer agents with probable inhibitory activity on the VEGFR-2 enzyme and on the expression of anti-apoptotic Bcl-2 and Bcl-xL proteins. The tested compounds were relatively safe against normal human fibroblasts (WI-38) and the cell proliferation of two examined cancer cell lines (HCT-116 and MCF-7) has been notably inhibited by all synthesised compounds with IC_{50} ranges from 7.8 to 32.0 μM against HCT-116 and from 7.2 to 24.0 μM against MCF-7, as compared to IC_{50} of 11.6 and 10.5 μM for sorafenib, respectively. In addition, compounds **1, 9, 10, 11, 12** and **15** showed excellent VEGFR-2 inhibitory activity. In particular, benzoxazoles **1** and **11** revealed to be slightly more or equally potent than sorafenib, with IC_{50} of 0.27, 0.36 μM and 0.35 μM, respectively. Moreover, docking studies showed that the compounds are positioned in a very similar manner to sorafenib into the VEGFR active site. Further mechanistic studies showed that compounds **1** and **11** induced apoptosis and inhibited the expression of anti-apoptotic Bcl-2 and Bcl-xL proteins in both HCT-116 and MCF-7 cancer cell lines. Finally, the high potency of this benzoxazole series suggested that conjugates **1** and **11** could avail as lead compounds for further investigation and optimisation to develop novel anti-proliferative agents, apoptotic inducers and inhibitors of Bcl-2/Bcl-xL expression.

4. Experimental

4.1. Chemistry

4.1.1. General

Melting points (°C) of the synthesised compounds were uncorrected and were measured using Electrothermal Stuart 5MP3.

Follow-up of reactions was performed using TLC plates of silica gel 60 F254 (Merck). The NMR spectrometric analyses have been recorded using Bruker-Avance 400 NMR spectrometer (400 MHz for ^{1}HNMR and100 MHz for ^{13}CNMR) in deuterated dimethylsulphoxide (DMSO-*d6*). Chemical shifts (δ_H) were reported relative to the solvent (DMSO-d_6). Mass spectra were recorded on Finnigan Mat SSQ 7000 mode EI 70 eV at the micro analytical unit, Cairo University, Cairo, Egypt. Schimadzu FT-IR 8400S spectrophotometer has been used for functional group analysis at the micro analytical unit, Cairo University, Cairo, Egypt. Elemental analyses were performed at the Regional Centre for Microbiology and Biotechnology, Al-Azhar University, Cairo, Egypt.

4.1.2. General methodology for preparation of the target compounds 1-12

In DMF (10 ml), a mixture of potassium salts **IIIa-c** (0.001 mol) and the convenient 4-(2-chloroacetamido)-*N*-(substituted) phenyl benzamide **VIIa-d** (0.001 mol), and KI (0.001 mol) was heated at 60 °C for 6 h. After completion of the reaction, the mixture was poured on crushed ice. The formed precipitates were filtered, dried, and recrystallized from methanol to afford the corresponding final target compounds **1–12**.

4.1.3. General methodology for preparation of the target compounds 13-15

In DMF (10 ml), a mixture of potassium salts **IIIa-c** (0.001 mol) and *N*-(4-(2-benzoyl-hydrazine-1-carbonyl)phenyl)-2-chloroacetamide **XI** (0.001 mol), and KI (0.001 mol) was heated at 60 °C for 6 h. After completion of the reaction, the mixture was poured on crushed ice. The formed precipitates were filtered, dried, and recrystallized from methanol to afford the corresponding final target compounds **13–15**.

Full characterisation (^{1}HNMR, ^{13}CNMR, IR, Mass spectrum and elemental analysis) data for novel compounds **1–15** have been presented in the Supplementary Materials.

4.2. Biological evaluation

All the procedures of the experiment utilised for biological evaluation in this article were performed as previously described; cytotoxicity[63,65], VEGFR-2 inhibitory activity[14], cell cycle analysis[66], Annexin V-FITC/PI apoptosis assay[67], and anti-apoptotic markers (Bcl-2, and Bcl-xL)[68,69]. All procedures were mentioned in detail in the Supplementary Materials.

4.3. Molecular docking

Virtual Molecular Docking studies were carried out using Molecular Operating Environment (MOE®) version 2015.10. The RCSB: Protein Data Bank was utilised to retrieve the crystal structure of Vascular Endothelial Growth Factor Receptor (VEGFR) co-crystallized with sorafenib (PDB ID: 4ASD) [70]. The downloaded protein was used for the docking study as a receptor and sorafenib was used as a reference drug.

Acknowledgements

The researcher Radwan El-Haggar is funded by a postdoctoral mission from the Ministry of Higher Education of the Arab Republic of Egypt.

Disclosure statement

No potential conflict of interest was reported by the author(s).

Funding

The author(s) reported there is no funding associated with the work featured in this article.

ORCID

Ibrahim H. Eissa http://orcid.org/0000-0002-6955-2263
Hazem A. Mahdy http://orcid.org/0000-0002-6620-241X
Nicolas Masurier http://orcid.org/0000-0001-9169-8149

References

1. Siegel RL, Miller KD, Jemal A. Cancer statistics, 2020. CA Cancer J. Clin 2020;70:1587–30.
2. Fabbro D, Parkinson D, Matter A. Protein tyrosine kinase inhibitors: new treatment modalities? Curr Opin Pharmacol 2002;2:374–81.
3. Wu C, Wang M, Tang Q, et al. Design, synthesis, activity and docking study of sorafenib analogs bearing sulfonylurea unit. Molecules 2015;20:19361–71.
4. Baudino TA. Targeted cancer therapy: the next generation of cancer treatment. Curr Drug Discov Technol 2015;12: 3–20.
5. Topcul M, Cetin I. Endpoint of cancer treatment: targeted therapies, Asian Pac. Asian Pac J Cancer Prev 2014;15: 4395–403.
6. Qin S, Li A, Yi M, et al. Recent advances on anti-angiogenesis receptor tyrosine kinase inhibitors in cancer therapy. J Hematol Oncol 2019;12:27–37.
7. Edlich F. BCL-2 proteins and apoptosis: recent insights and unknowns. Biochem Biophys Res Commun 2018;500:26–34.
8. Hata AN, Engelman JA, Faber AC. The BCL2 family: key mediators of the apoptotic response to targeted anticancer therapeutics. Cancer Discov 2015;5:475–87.
9. Marone M, Ferrandina G, Macchia G, et al. Bcl-2, Bax, Bcl-x(L) and Bcl-x(S) expression in neoplastic and normal endometrium. Oncology 2000;58:161–8.
10. Lugano R, Ramachandran M, Dimberg A. Tumor angiogenesis: causes, consequences, challenges and opportunities. Cell Mol Life Sci 2020;77:1745–70.
11. Folkman J. Angiogenesis in cancer, vascular, rheumatoid and other disease. Nat Med 1995;1:27–31.
12. Karamysheva AF. Mechanisms of angiogenesis. Biochemistry 2008;73:751–62.
13. Kerbel RS. Tumor angiogenesis: past, present and the near future. Carcinogenesis 2000;21:505–15.
14. Ahmed MF, Santali EY, El-Haggar R. Novel piperazine-chalcone hybrids and related pyrazoline analogs targeting VEGFR-2 kinase; design, synthesis, molecular docking studies, and anticancer evaluation. J. Enzy. Inhib. Med. Chem 2021;36:307–18.
15. Modi SJ, Kulkarni VM. Vascular Endothelial Growth Factor Receptor (VEGFR-2)/KDR inhibitors: medicinal chemistry perspective. Med Drug Discov 2019;2:100009.
16. Potashman MH, Bready J, Coxon A, et al. Design, synthesis, and evaluation of orally active benzimidazoles and benzoxazoles as vascular endothelial growth factor-2 receptor tyrosine kinase inhibitors. J Med Chem 2007;50:4351–73.

17. Yuan X, Yang Q, Liu T, et al. Design, synthesis and in vitro evaluation of 6-amide-2-aryl benzoxazole/benzimidazole derivatives against tumor cells by inhibiting VEGFR-2 kinase. Eur J Med Chem 2019;179:147–65.
18. DR, Green Means to an end: apoptosis and other cell death mechanisms. New York: Cold Spring Harbor, Cold Spring Harbor Laboratory Press; 2011.
19. Spierings D, McStay G, Saleh M, et al. Connected to death: the (unexpurgated) mitochondrial pathway of apoptosis. Science 2005;310:66–7.
20. Wang B, Xu A. Aryl hydrocarbon receptor pathway participates in myocardial ischemia reperfusion injury by regulating mitochondrial apoptosis. Med Hypotheses 2019;123:2–5.
21. Modugno M, Banfi P, Gasparri F, et al. Mcl-1 antagonism is a potential therapeutic strategy in a subset of solid cancers. Exp Cell Res 2015;332:267–77.
22. Placzek WJ, Wei J, Kitada S, et al. A survey of the anti-apoptotic Bcl-2 subfamily expression in cancer types provides a platform to predict the efficacy of Bcl-2 antagonists in cancer therapy. Cell Death Dis 2010;1:e40.
23. Eldehna WM, Abo-Ashour MF, Al-Warhi T, et al. Development of 2-oxindolin-3-ylidene-indole-3-carbohydrazide derivatives as novel apoptotic and anti-proliferative agents towards colorectal cancer cells. J Enzy Inhib Med Chem 2021;36:319–28.
24. Sabt A, Abdelhafez OM, El-Haggar RS, et al. Novel coumarin-6-sulfonamides as apoptotic anti-proliferative agents: synthesis, in vitro biological evaluation, and QSAR studies. J Enzyme Inhib Med Chem 2018;33:1095–107.
25. Chen G, Liu Z, Zhang Y, et al. Synthesis and anti-inflammatory evaluation of novel benzimidazole and imidazopyridine derivatives. ACS Med Chem Lett 2013;4:69–74.
26. Kakkar S, Narasimhan B. A comprehensive review on biological activities of oxazole derivatives. BMC Chem 2019;13: 1–24.
27. Mohamed MS, Rashad AE, Adbel-Monem M, Fatahalla SS. New anti-inflammatory agents. Z Naturforsch C J Biosci 2007;62:27–31.
28. Veerasamy R, Roy A, Karunakaran R, Rajak H. Structure-activity relationship analysis of benzimidazoles as emerging anti-inflammatory agents: an overview. Pharmaceuticals 2021;14: 663–93.
29. Seth K, Garg SK, Kumar R, et al. Chakraborti, 2-(2-Arylphenyl)benzoxazole As a Novel Anti-Inflammatory Scaffold: Synthesis and Biological Evaluation. ACS Med Chem Lett 2014;5:512–6.
30. Balaswamy G, Pradeep P, Srinivas K, Rajakomuraiah T. Synthesis, characterization and anti-microbial activity of new series of benzoxazole derivatives. Int J Chem Sci 2012;10: 1830–6.
31. Gamba E, Mori M, Kovalenko L, et al. Identification of novel 2-benzoxazolinone derivatives with specific inhibitory activity against the HIV-1 nucleocapsid protein. Eur J Med Chem 2018;145:154–64.
32. Rida SM, Ashour FA, El-Hawash SA, et al. Synthesis of some novel benzoxazole derivatives as anticancer, anti-HIV-1 and antimicrobial agents. Eur J Med Chem 2005;40:949–59.
33. Zeyrek CT, Arpacı ÖT, Arısoy M, Onurdağ FK. Synthesis, antimicrobial activity, density functional modelling and molecular docking with COVID-19 main protease studies of benzoxazole derivative: 2-(p-chloro-benzyl)-5-[3-(4-ethly-1-piperazynl) propionamido]-benzoxazole. J Mol Struct 2021; 1237:130413.
34. Bhole RP, Chikhale RV, Wavhale RD, et al. Design, synthesis and evaluation of novel enzalutamide analogues as potential anticancer agents. Heliyon 2021;7:e06227.
35. Bradshaw TD, Westwell AD. The development of the antitumour benzothiazole prodrug, Phortress, as a clinical candidate. Curr Med Chem 2004;11:1009–21.
36. Dadashpour S, Kucukkilinc TT, Ercan A, et al. Synthesis and anticancer activity of benzimidazole/benzoxazole substituted triazolotriazines in hepatocellular carcinoma. Anticancer Agents Med Chem 2019;19:2120–9.
37. Desai S, Desai V, Shingade S. In-vitro Anti-cancer assay and apoptotic cell pathway of newly synthesized benzoxazole-N-heterocyclic hybrids as potent tyrosine kinase inhibitors. Bioorg Chem 2020;94:103382.
38. Dhadda S, Kumar A, Kamlesh R, et al. Benzothiazoles: From recent advances in green synthesis to anti-cancer potential. Sustain Chem Phar 2021;24:100521.
39. Eldehna WM, El Hassab MA, Abo-Ashour MF, et al. Development of isatin-thiazolo[3,2-a]benzimidazole hybrids as novel CDK2 inhibitors with potent in vitro apoptotic anti-proliferative activity: Synthesis, biological and molecular dynamics investigations. Bioorg Chem 2021;110:104748.
40. El-Hady HA, Abubshait SA. Synthesis and anticancer evaluation of imidazolinone and benzoxazole derivatives. Arab J Chem 2017;10:S3725–S3731.
41. El-Hameed RHA, Fatahala SS, Sayed AI. Synthesis of some novel benzimidazole derivatives as anticancer agent, and evaluation for CDK2 inhibition activity. Med Chem 2022;18: 1–11.
42. Mantzourani C, Gkikas D, Kokotos A, et al. Synthesis of benzoxazole-based vorinostat analogs and their antiproliferative activity. Bioorg Chem 2021;114:105132.
43. Osmaniye D, Korkut Çelikateş B, Sağlık BN, et al. Synthesis of some new benzoxazole derivatives and investigation of their anticancer activities. Eur J Med Chem 2021;210:112979.
44. Xiang P, Zhou T, Wang L, et al. Novel benzothiazole, benzimidazole and benzoxazole derivatives as potential antitumor agents: synthesis and preliminary in vitro biological evaluation. Molecules 2012;17:873–83.
45. Khajondetchairit P, Phuangsawai O, Suphakun P, et al. Design, synthesis, and evaluation of the anticancer activity of 2-amino-aryl-7-aryl-benzoxazole compounds. Chem Biol Drug Des 2017;90:987–94.
46. Eskander RN, Tewari KS. Incorporation of anti-angiogenesis therapy in the management of advanced ovarian carcinoma-mechanistics, review of phase III randomized clinical trials, and regulatory implications. Gynecol Oncol 2014;132: 496–505.
47. Lee K, Jeong KW, Lee Y, et al. Pharmacophore modeling and virtual screening studies for new VEGFR-2 kinase inhibitors. Eur J Med Chem 2010;45:5420–7.
48. Xie QQ, Xie HZ, Ren JX, et al. Pharmacophore modeling studies of type I and type II kinase inhibitors of Tie2. J Mol Graph Model 2009;27:751–8.
49. Machado VA, Peixoto D, Costa R, et al. Synthesis, antiangiogenesis evaluation and molecular docking studies of 1-aryl-3-[(thieno[3,2-b]pyridin-7-ylthio)phenyl]ureas: Discovery of a new substitution pattern for type II VEGFR-2 Tyr kinase inhibitors. Bioorg Med Chem 2015;23:6497–509.

50. Wang Z, Wang N, Han S, et al. Dietary compound isoliquiritigenin inhibits breast cancer neoangiogenesis via VEGF/VEGFR-2 signaling pathway. PLoS One 2013;8:e68566.
51. Dietrich J, Hulme C, Hurley LH. The design, synthesis, and evaluation of 8 hybrid DFG-out allosteric kinase inhibitors: a structural analysis of the binding interactions of Gleevec, Nexavar, and BIRB-796. Bioorg Med Chem 2010;18:5738–48.
52. Kaul S, Kumar A, Sain B, Bhatnagar AK. Simple and Convenient One-Pot Synthesis of Benzimidazoles and Benzoxazoles using N,N-Dimethylchlorosulfitemethaniminium Chloride as Condensing Agent. Synthetic Commun 2007;37:2457–60.
53. Alsaif NA, Dahab MA, Alanazi MM, et al. New quinoxaline derivatives as VEGFR-2 inhibitors with anticancer and apoptotic activity: design, molecular modeling, and synthesis. Bioorg Chem 2021;110:104807.
54. Alanazi MM, Elkady H, Alsaif NA, et al. New quinoxaline-based VEGFR-2 inhibitors: design, synthesis, and antiproliferative evaluation with in silico docking, ADMET, toxicity, and DFT studies. RSC Adv 2021;11:30315–28.
55. Alanazi MM, Eissa IH, Alsaif NA, et al. Design, synthesis, docking, ADMET studies, and anticancer evaluation of new 3-methylquinoxaline derivatives as VEGFR-2 inhibitors and apoptosis inducers. J Enzyme Inhib Med Chem 2021;36:1760–82.
56. Alsaif NA, Taghour MS, Alanazi MM, et al. Discovery of new VEGFR-2 inhibitors based on bis([1, 2, 4]triazolo)[4,3-a:3′,4′-c]quinoxaline derivatives as anticancer agents and apoptosis inducers. J Enzyme Inhib Med Chem 2021;36:1093–114.
57. El-Zahabi MA, Sakr H, El-Adl K, et al. Design, synthesis, and biological evaluation of new challenging thalidomide analogs as potential anticancer immunomodulatory agents. Bioorg Chem 2020;104:104218.
58. Chikhale R, Thorat S, Choudhary RK, et al. Design, synthesis and anticancer studies of novel aminobenzazolyl pyrimidines as tyrosine kinase inhibitors. Bioorg Chem 2018;77:84–100.
59. Stevens MF, McCall CJ, Lelieveld P, et al. Structural studies on bioactive compounds. 23. Synthesis of polyhydroxylated 2-phenylbenzothiazoles and a comparison of their cytotoxicities and pharmacological properties with genistein and quercetin. J Med Chem 1994;37:1689–95.
60. Ghoshal T, Patel TM. Anticancer activity of benzoxazole derivative (2015 onwards): a review. Fut J Pharm Sci 2020;6:94–113.
61. Omar AME, AboulWafa OM, El-Shoukrofy MS, Amr ME. Benzoxazole derivatives as new generation of anti-breast cancer agents. Bioorg Chem 2020;96:103593.
62. Peng F, Liu D, Zhang Q, et al. VEGFR-2 inhibitors and the therapeutic applications thereof: a patent review (2012-2016). Expert Opin Ther Pat 2017;27:987–1004.
63. Skehan P, Storeng R, Scudiero D, et al. New colorimetric cytotoxicity assay for anticancer-drug screening. J Natl Cancer Inst 1990;82:1107–12.
64. Meng XY, Zhang HX, Mezei M, Cui M. Molecular docking: a powerful approach for structure-based drug discovery. Curr Comput Aided Drug Des 2011;7:146–57.
65. Omar AM, El-Araby ME, Abdelghany TM, et al. Introducing of potent cytotoxic novel 2-(aroylamino)cinnamamide derivatives against colon cancer mediated by dual apoptotic signal activation and oxidative stress. Bioorg Chem 2020;101:103953.
66. Wang J, Lenardo MJ. Roles of caspases in apoptosis, development, and cytokine maturation revealed by homozygous gene deficiencies. J Cell Sci 2000;113:753–7.
67. Lo KK, Lee TK, Lau JS, et al. Luminescent biological probes derived from ruthenium(II) estradiol polypyridine complexes. Inorg Chem 2008;47:200–8.
68. Aborehab NM, Elnagar MR, Waly NE. Gallic acid potentiates the apoptotic effect of paclitaxel and carboplatin via overexpression of Bax and P53 on the MCF-7 human breast cancer cell line. J Biochem Mol Toxicol 2021;35:e22638.
69. Burnette WN. "Western blotting": electrophoretic transfer of proteins from sodium dodecyl sulfate-polyacrylamide gels to unmodified nitrocellulose and radiographic detection with antibody and radioiodinated protein A. Anal Biochem 1981;112:195–203.
70. Available from: http://www.rcsb.org/